

# Chapter 21

## Multiscale Molecular Modeling

Matej Praprotnik and Luigi Delle Site

### Abstract

We review the basic theoretical principles of the adaptive resolution simulation scheme (AdResS). This method allows to change molecular resolution on-the-fly during a simulation by changing the number of degrees of freedom in specific regions of space where the required resolution is higher than in the rest of the system. We also report about recent extensions of the method to the continuum and quantum regimes.

**Key words:** Multiscale modeling, Adaptive resolution simulation, AdResS

---

### 1. Introduction

Many problems in condensed matter, material science, and chemistry are multiscale in nature, meaning that the interplay between different scales plays a fundamental role. An exhaustive description of the related physical phenomena requires, from a theoretical or computational point of view, the simultaneous treatment of all the scales involved. This is a prohibitive task not only because of the large computational resources required but above all because the large amount of data produced would mostly contain information not essential to the problem analyzed; actually they may overshadow the underlying fundamental physics or chemistry of the system. A solution to this problem is that of treating the problems via multiscale approaches. In this case one simplifies the model of the physical system to the largest extent possible while keeping all the necessary details of the system where this is required. Multiscale methods have been developed and successfully applied to study solid state systems, where the atomistic models were either combined with the finite elements method (1–5) or linked to a quantum mechanical model (6, 7). In particular, for some systems (e.g., the solvation of a molecule) some regions (the first two or three solvation shells

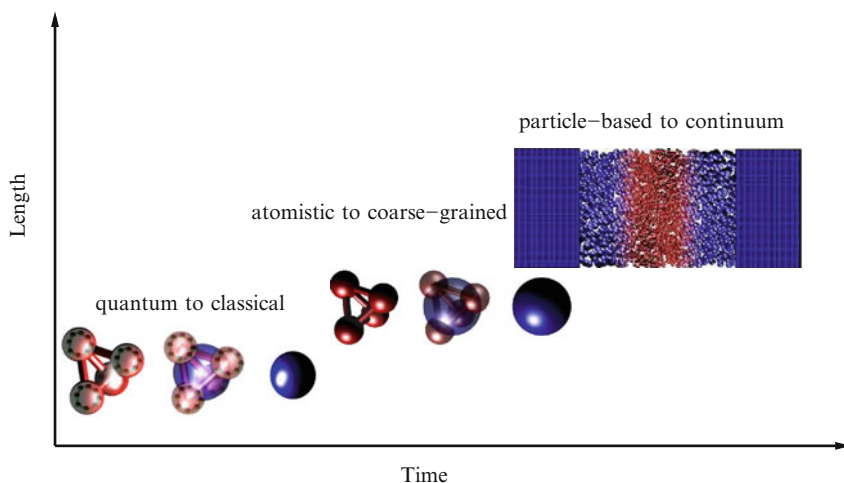


Fig. 1. Multiscale modeling: concurrent couplings. At the smallest scale the coupling is between the quantum and the classical (or coarse-grained) molecular resolution. The quantum resolution is here represented by the path-integral/polymering representation of atoms (8). Going to a larger scale, one goes from the atomistic to the coarse-grained resolution(9) and finally at mesoscopic/macrosopic scales one couples particle-based representations to the continuum(10).

around the solute) require a higher resolution than the rest, but at the same time, because of the large fluctuations, an open boundary between the regions is required so that there is free exchange of particles. For that one requires adaptive resolution simulation schemes (see Fig. 1) which allow molecules to change resolution according to the region where they are instantaneously located. From a technical point of view, this means that the space is partitioned in regions characterized by different molecular resolutions where molecules can freely diffuse, changing their representation while keeping the overall thermodynamic equilibrium of the system (11, 12). The aim of this chapter is to review an adaptive simulation method, the adaptive resolution simulation (AdResS) method (9, 13), which has been shown to be particularly robust in coupling scales from the quantum to the classical atomistic up to the continuum (8, 14, 15).

## 2. Adaptive Resolution Simulation

### 2.1. Theoretical Framework

In this section we report the basic theoretical principles employed in the development of the AdResS. Let us consider a liquid of  $N$  molecules in a simulation box with a volume  $V$ , which is divided into two equally large domains  $A$  and  $B$ . In the domain  $A$ , we represent molecules on a low-resolution level, while the domain  $B$  is described using a higher resolution representation, for example, all-atom resolution. The number  $n$  of degrees of freedom (DOFs)

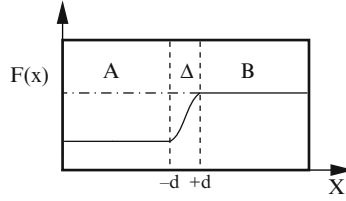


Fig. 2. Free energy density profile across the simulation box.

per molecule, which we explicitly treat in our description, is hence lower in the coarse-grained domain  $A$  and higher in the all-atom domain  $B$ . The two domains are in thermodynamic equilibrium and freely exchanging molecules, that is, the liquid is homogeneous across the whole simulation box. The necessary boundary condition for the thermodynamic equilibrium between the two representations is

$$\mu_A = \mu_B, \quad p_A = p_B, \quad T_A = T_B, \quad (1)$$

where  $\mu_A$ ,  $p_A$ , and  $T_A$ , and  $\mu_B$ ,  $p_B$ , and  $T_B$  are the chemical potentials, pressures, and temperatures of the liquid in the both domains, respectively (9, 11, 16). The question that arises at this point is how to achieve that the condition (1) is satisfied within a molecular dynamics simulation where the liquid has the same structure on both sides if analyzed on the lower resolution level. In an attempt to answer this question, we plot in Fig. 2 the free-energy density  $F = F(x)$  profile of the system associated to the DOFs that we explicitly consider in the simulation. Since the free energy is an extensive quantity, its value is lower in the domain  $A$  because the number of DOFs  $n_A$  is lower than in the domain  $B$ . For a smooth transition between the two resolutions, we introduce a transition regime  $\Delta$  (9) at the interface where the molecules slowly change their representation. In this regime they are in equilibrium with their actual surrounding and change continuously until the region of the new representation is reached. The molecules “arrive” fully equilibrated into the surrounding described by the new representation. The number of explicitly treated DOFs is  $n = n(x)$  with  $n_A = \text{const}_A$ ;  $n_B = \text{const}_B$ ; and  $n_A = n(x)$ . The system is in equilibrium which implies  $\lim_{x \rightarrow d^-} \frac{\partial F_A(x)}{\partial x} = \lim_{x \rightarrow d^+} \frac{\partial F_B(x)}{\partial x} = 0 \implies \lim_{x \rightarrow d^-} \frac{\partial n_A(x)}{\partial x} = \lim_{x \rightarrow d^+} \frac{\partial n_B(x)}{\partial x} = 0$ , and  $\partial F_A / \partial N_A + \phi = \mu_A$  and  $\partial F_B / \partial N_B = \mu_B$ , where  $\phi$  is the free energy per molecule associated with the integrated out DOFs. In the adaptive resolution scheme presented here, we do not book-keep the integrated out DOFs in the coarse-grained models. Rather, we reduce the many-body potential of the higher resolution representation into a reduced effective potential and keep only two-body terms. We do not treat explicitly the one-body terms, which depend only on the temperature (17), and hence do not contribute to the intermolecular forces.

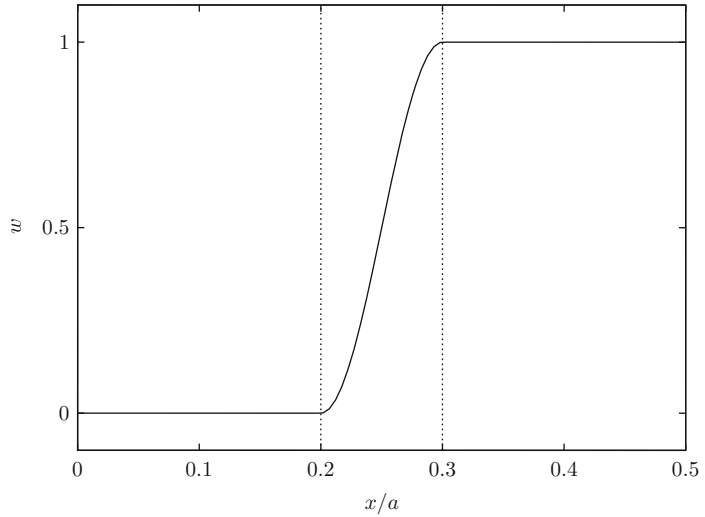


Fig. 3. The weighting function.

Instead, they can be viewed, in the adaptive scheme, as the equivalent of a latent heat. As explained later, in our model this part of the free energy is supplied or removed by a local thermostat. Of course, if we explicitly book-kept the one-body terms (three-body and higher terms are also omitted for numerical efficiency) in the effective potential, the free-energy profile would be flat across the whole simulation box (the dashed line in Fig. 2) (17) (P. Español, 2010, private communication). The free-energy density profile allows us to define a weighting function which has certain similarities with an order parameter (9). The weighting function  $w$  that determines the level of resolution across the system is presented in Fig. 3. It is introduced in such a way that  $w = 1$  and  $w = 0$  correspond to the high- and low-resolution regions, respectively, while the values  $0 < w < 1$  correspond to the transition regime. Thus, crossing the transition regime, the number of DOFs changes in a continuous manner. The change of resolution can be seen as a change in the dimensionality of the phase space of the switching DOF. If the particular DOF is fully considered ( $w = 1$ ), then the phase space has its full dimensionality. On the other hand, if it is completely switched off ( $w = 0$ ), it does not contribute to any statistical average, and thus, its dimensionality is zero. In the transition regime, the partially switched-on DOF contributes to statistical averages according to its weight  $w$ . To properly mathematically describe the continuous change of the phase space dimensionality and define thermodynamic properties, for example, temperature, in the transition regime, we resort to fractional calculus (18–22) and divide the transition regime into thin slabs, each with the different values  $w$  between 0 and 1.

For the fractional quadratic DOF  $p$  with the weight  $w$ , we can then write the partition function as

$$\begin{aligned}
\exp(-\beta F_p) &= C \int \exp(-\beta p^2/2) dV_w \\
&= 2C \int_0^\infty \exp(-\beta p^2/2) |p|^{w-1} \frac{dp}{\Gamma(w)} \\
&= \frac{2^{w/2} C \Gamma(w/2)}{\Gamma(w)} \beta^{-w/2} \sim \beta^{-w/2}, \tag{2}
\end{aligned}$$

where we introduced the infinitesimal volume element of the fractional configurational space defined as  $dV_w = |p|^{w-1} dp / \Gamma(w) = dp^w / (w\Gamma(w))$ . Here  $\Gamma$  is the gamma function (16). It directly follows  $\langle K_w \rangle = \frac{d(\beta F_p)}{d\beta} = \frac{w}{2\beta} = \frac{wk_B T}{2}$ , where  $\langle K_w \rangle$  is the average kinetic energy per fractional quadratic DOF with the weight  $w$ . This is a generalization of the equipartition principle to non-integer quadratic DOFs (16, 23). In equilibrium  $T_A = T_B = T_\Delta = T$ , and thus,  $n_w \sim w$ . Using this framework the temperature in the transition region is correctly defined. This enables us to employ the local thermostat to control the free-energy difference between the two levels of resolution (24). The corresponding free energy for a generic quadratic switchable DOF  $p$  is (12)

$$F_p = \mu_p^{kin}(w) = -kT \log \left[ \int e^{-\beta p^2} d^w p \right], \tag{3}$$

and hence, the total explicit contribution of the entire set of switchable DOFs per molecule is

$$\mu^{kin}(w) = \sum_{DOF} \mu_p^{kin}(w). \tag{4}$$

The kinetic component to  $\phi$ , that is, the latent heat (in principle one could also include the quadratic intramolecular potential terms (17)), is<sup>1</sup>

$$\phi(w)^{kin} = \mu_B^{kin} - \mu^{kin}(w). \tag{5}$$

The analytical solution of Eq. 3 is:

$$\mu_p^{kin}(w) \sim CkT \left(\frac{w}{2}\right) \log(T) \tag{6}$$

where  $C$  is a constant,  $k$  the Boltzmann constant, and  $T$  is the temperature. Equation 6 is the ideal gas kinetic contribution to the chemical potential coming from the internal DOFs. Usually in a simulation with single-resolution representation of the molecules, this contribution to the chemical potential is ignored being only a trivial constant depending only on temperature (17). In our case, where the DOFs of interest might continuously change in going from

<sup>1</sup>As defined by Eqs. 3 and 4,  $\mu^{kin}(0) \neq \mu_A^{kin}$ . In fact,  $\mu_A^{kin} = \mu^{kin}(0) + \phi(0)^{kin} = \mu_B^{kin}$ .  $\mu^{kin}(w)$  represents only the contribution of the switched-on DOFs to the kinetic part of chemical potential. The rest is included in  $\phi(w)^{kin}$ .

one representation to another, each DOF in the transition region contributes differently according to the corresponding value of  $w(x)$ . Thus, the latent heat defined by Eq. 5 is crucial for keeping the thermodynamic equilibrium between two levels of resolution in the adaptive resolution simulations. The kinetic part of the free energy depends in the first order linearly on  $w$ , which determines the slope of the free-energy density profile in the transition regime in Fig. 2.

Next, we shall couple the two levels of resolution in a molecular dynamics approach: AdResS is built on a force-based approach (11). The interpolation formula for the pair force between molecules  $\alpha$  and  $\beta$  writes as

$$\mathbf{F}_{\alpha\beta} = w(X_\alpha)w(X_\beta)\mathbf{F}_{\alpha\beta}^B + [1 - w(X_\alpha)w(X_\beta)]\mathbf{F}_{\alpha\beta}^A \quad (7)$$

where  $\mathbf{F}_{\alpha\beta}^A$  is the force obtained from the potential of representation  $A$ , and  $\mathbf{F}_{\alpha\beta}^B$ , the one obtained from the potential of representation  $B$ ;  $w(X)$  is the switching function and depends on the center of mass positions  $X_\alpha$  and  $X_\beta$ , of the two interacting molecules. The basic idea of the scheme given by Eq. 7 is to enable the molecule to find its correct orientation in the liquid once it is given a random orientation at the low-resolution/transition regime boundary (9). Even though there might be some overlaps with neighboring molecules, the atomistic interactions are turned off ( $w = 0$ ) at that boundary. As the molecule approaches to the high-resolution regime, the atomistic interactions are gradually turned on, and the molecule on-the-fly finds its proper orientation. As it turns out, it is important to interpolate the forces and not the interaction potentials in order to satisfy Newton's third law (16, 23, 25). This is crucial for the local linear momentum conservation and proper diffusion of molecules across the transition regime. Each time a molecule leaves (or enters) the coarse-grained region, it gradually gains (or loses) its vibrational and rotational DOFs while retaining its linear momentum. The change in resolution carried out by AdResS is not time reversible as a given molecule in the low-resolution domain  $A$  corresponds to many orientations and configurations of the corresponding molecule in the high-resolution domain  $B$  (15). Since time reversibility is essential for energy conservation (26), AdResS does not conserve energy. In particular, the force in Eq. 7 is in general not conservative in the transition region (i.e., in general  $\oint \mathbf{F}_{\alpha\beta} \cdot d\mathbf{r} \neq 0$ ) (23, 25). Hence, to supply or remove the latent heat associated with the switch of resolution (see Eq. 5), we use a DPD thermostat (24, 27). The thermostat forces do not enter into the AdResS interpolating scheme, Eq. 7, instead they are added to the AdResS (9).

Using properly derived effective pair interactions  $\mathbf{F}_{\alpha\beta}^A$  (see Sect. 2), the boundary conditions as given by Eq. 1 are satisfied. The AdResS scheme (7) has been successfully applied to a liquid of tetrahedral molecules (9, 13), a generic macromolecule in solvent (28), and liquid water (14, 29). As already stated, to perform adaptive resolution simulations requires equilibrium between the

different regimes, which is facilitated by a transition zone. However, the necessary condition for thermodynamic equilibrium between two different representations as well as the transition zone, that is, the chemical potential, pressure, and temperature equivalence, can in some complex systems not be assured by a mere derivation of the effective pair interactions between coarse-grained molecules. Furthermore, one can also consider situations where we interface different molecular models at the same level of resolution (e.g., flexible and rigid atomistic water) with free, unhindered exchange of molecules among the regions of different molecular representation. A barrier free exchange of molecules over the border lines of molecular resolution is required to properly account for fluctuations. The number of DOFs in such cases remains the same, but forces acting on each atom are different in the different regions. To treat these scenarios, we recently introduced a generalization of AdResS (12), which allows to couple rather loosely connected molecular representations, that is, it maintains two different representations with, in general, different chemical potentials ( $\mu_A \neq \mu_B$ ) in thermodynamic equilibrium. In the generalized approach, we extend the original scheme, Eq. 7, by subtracting a thermodynamic force  $\mathbf{F}^{TD}$ . The total, force on molecule  $\alpha$  is after subtracting a thermodynamic force  $\mathbf{F}^{TD}$ ,

$$\mathbf{F}_\alpha = \sum_{\beta \neq \alpha} \left( w(X_\alpha) w(X_\beta) \mathbf{F}_{\alpha\beta}^B + [1 - w(X_\alpha) w(X_\beta)] \mathbf{F}_{\alpha\beta}^A \right) - \mathbf{F}^{TD}(X_\alpha) \quad (8)$$

where  $F_x^{TD} = -\frac{\partial \mu^{exc}}{\partial x}$  and  $\mu^{exc}$  is the excess chemical potential due to the intermolecular interactions (12). AdResS is a nonconservative scheme, and hence, the potential is not defined in the transition regime. Therefore, to calculate numerically the excess chemical potential, we proceed as follows. We divide the simulation box into regions of force fields  $A$  and  $B$  and the transition region in between. The region  $A$  is characterized by the value of the switching function  $w_0 = 0$ . The region  $B$  is characterized by the value of the switching function  $w_{N+1} = 1$ . In the transition regime, the value of  $w$  in the actual simulations varies continuously. Here we approximate this by discretizing  $w$  into  $N$  steps  $w_1, w_2, \dots, w_{N-1}, w_N$ . For any fixed value of  $w^2$ , the energy function is well-defined, and the excess chemical potential then is defined as  $\mu^{exc}(x_i) = \mu_{w_i}^{exc}$ , where the  $\mu_{w_i}^{exc}$  is the chemical potential of the molecules in a bulk system of the specific representation of  $w_i$ . To calculate numerically each  $\mu^{exc}(w_i)$ , one can use standard particle insertion methods. Repeating this procedure with all values of  $w_i$  leads to a position-dependent excess chemical potential  $\mu^{exc}(x)$ , which represent the second contribution to  $\phi$  (12).

---

<sup>2</sup>This is the value that one obtains by using the insertion methods in a hybrid system exclusively composed of hybrid molecules with a fixed level of resolution  $0 \leq w = w(x) = const. \leq 1$  corresponding to a fixed bulk value  $\mu_{w(x)}$ .

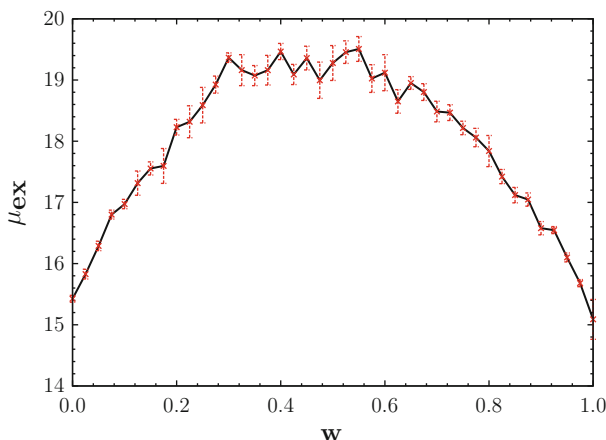


Fig. 4. The excess chemical potential. Reprinted with permission from (12). Copyright 2010, American Institute of Physics.

As a test case, we applied the above generalized scheme to a liquid of tetrahedral molecules (12). An intrinsic, though numerically negligible, problem in the original formulation of AdResS was the fact that we found some evident (but small) density variations through the transition regime due to the linear interpolation of forces in AdResS (13). We showed that employing the above derived scheme and introducing the corresponding thermodynamic force this problem can be solved. Figure 4 shows  $\mu^{exc}$ . The system is set up in such a way that the equation of state is the same in both the coarse-grained and all atom regimes at the temperature and density of the current simulation. Because of that,  $\mu^{exc}(x)$  is the same for  $w = 1$  and for  $w = 0$ . The resulting  $F_x^{TD}$  and the density profile are depicted in Fig. 5. The application of the thermodynamic force flattens the artificial density fluctuations by preserving the thermodynamic equilibrium between the two levels of resolution.

## 2.2. Mapping of Structural Properties

As discussed in the previous section, we have to map the structure of the low-resolution representation as close as possible to the reference high-resolution counterpart. This is necessary because we want the molecules to adapt, when they enter the high-resolution domain from the low-resolution region (through the transition one), as quickly as possible to the new environment. To this end, we reduce the many-body potential of the higher resolution representation into a reduced effective potential (30) using any of the standard methods, for example, iterative Boltzmann inversion (31–33), an iterative inverse statistical mechanics approach (34), force-matching scheme (35, 36), extended ensemble approach (37, 38). For more details of these methods, we refer the reader to the chapter by William G. Noid. Note that due to numerical efficiency, we consider only pair effective interactions and omit the higher or one-body

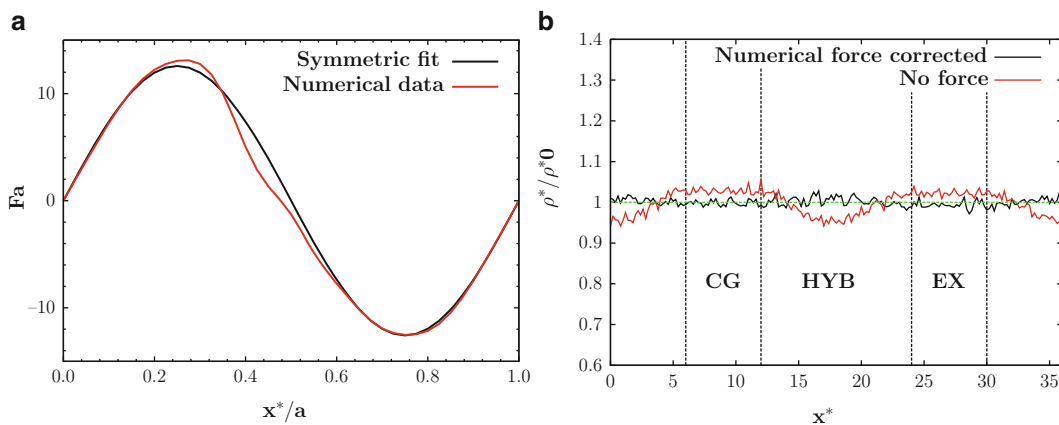


Fig. 5. Application of the thermodynamic force—reducing the density fluctuations in the transition regime. Reprinted with permission from (12). Copyright 2010, American Institute of Physics. (a) Thermodynamic force (b) Density across the simulation box.

terms (see the Section 1). Another issue is also whether to match the pressure or compressibility of the models. One can namely not match both (39). We need pressure equality to satisfy equilibrium condition (1), but on the other hand, the models should have the same compressibility in order to have the same thermodynamic fluctuations. To circumvent this problem, we resort here to the generalized AdResS scheme, Eq. 8, where via the effective potential we assure the same compressibility of the models while using the thermodynamic force we guarantee the equilibrium between the two levels of resolution.

As it turns out, AdResS is quite robust against the details of the low-resolution model, and we do not need to map the radial distribution functions exactly to the linethickness. This was demonstrated in the case of liquid water (15) where a non-perfect effective potential was deliberately used to study the robustness of the method, as depicted in Fig. 6.

### 2.3. Mapping of Dynamical Properties

Having mapped the structural properties via the effective potential derivation, one typically loses the control over dynamical properties of coarse-grained models. Due to soft effective interactions, the transport coefficient of the coarse-grained models differs quite substantially from the reference atomistic values, that is, diffusion constants and viscosities are too high/low, respectively. In our approach in order to match the dynamics of both levels of resolution, we slow down the dynamics of coarse-grained models using position-dependent local thermostats, as described below.

#### 2.3.1. Position Dependent Langevin Thermostat

If one is not concerned about hydrodynamics, one can use the stochastic Langevin thermostat where the transport coefficient is tuned by changing the strength of the coupling with the

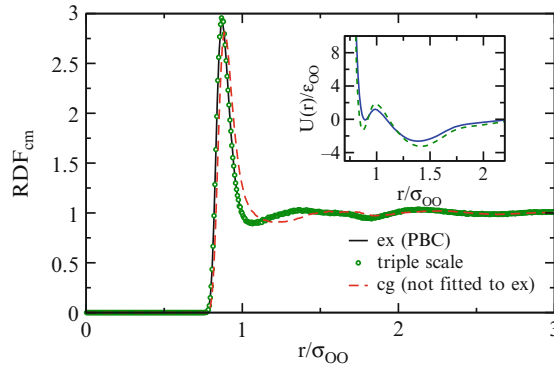


Fig. 6. RDFs and corresponding effective pair potential for water. Reprinted with permission from (15). Copyright 2009, American Institute of Physics.

thermostat. The Langevin equation with a position dependent coefficient  $\Gamma(x)$  can be written as (29)

$$m_i dv_i/dt = F_i - m_i \Gamma(x) v_i + R_i(x, t) \tag{9}$$

where  $R_i(x, t)$  is

$$\langle R_i(x, t) \rangle = 0, \tag{10}$$

$$\langle R_i(x, t_1) R_j(x, t_2) \rangle = 2\Gamma(x) m_i kT \delta(t_1 - t_2) \delta_{ij} \tag{11}$$

$$\Gamma(w) = \begin{cases} \Gamma_{cg} & \text{if } w \leq 0.6 \\ \alpha w + \beta & \text{if } 0.6 < w \leq 1.0. \end{cases} \tag{12}$$

This choice provides a simple interpolation between the two limit values of  $\Gamma(0.6) = \Gamma(0) = \Gamma_{cg} = 15 \text{ ps}^{-1}$  and  $\Gamma(1) = \Gamma_{all-atom} = 5 \text{ ps}^{-1}$ . The parameters  $\alpha$  and  $\beta$  are  $-25 \text{ ps}^{-1}$  and  $30 \text{ ps}^{-1}$ , respectively. In the adaptive resolution simulations, the force  $F_i$  is defined by the AdResS scheme. The results depicted in Fig. 7 clearly show that by employing our position dependent Langevin thermostat, we effectively slow down the dynamics of the coarse-grained models to be equal to the reference atomistic one.

2.3.2. Transverse  
DPD Thermostat

We have shown in the previous example that the coarse-grained dynamics can be slowed down by increasing the effective friction in the coarse-grained system using the position-dependent Langevin thermostat. However, it is well-known that the Langevin thermostat does not reproduce the correct hydrodynamics, that is, the hydrodynamic interactions are nonphysically screened. To correctly describe hydrodynamic interactions, one has to resort to the dissipative particle dynamics (DPD) thermostat. For tuning the transport coefficient of liquids, we extended the standard DPD thermostat (27) by including the damping of the transverse components of the relative velocity, yet keeping the advantages of conserving Galilei invariance and within our error bar also hydrodynamics (24).

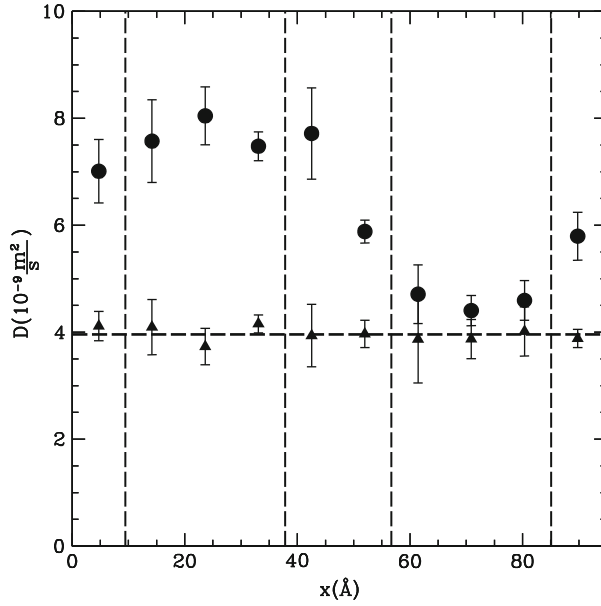


Fig. 7. Diffusion constant profile using the standard and position dependent Langevin thermostats. Reprinted with permission from (29). Copyright 2008, American Institute of Physics.

The Transverse DPD thermostat is introduced as follows (24):

$$\dot{\vec{p}}_i = \vec{F}_i^C + \vec{F}_i^D + \vec{F}_i^R, \quad (13)$$

where the first, second, and third term on the RHS denote conservative, damping, and random forces, respectively (40). The damping and random forces are expressed as:

$$\vec{F}_{ij}^D = -\zeta w^D(r_{ij}) \overset{\leftrightarrow}{P}_{ij}(\vec{r}_{ij}) \vec{v}_{ij}, \quad (14)$$

$$\vec{F}_{ij}^R = \sigma w^R(r_{ij}) \overset{\leftrightarrow}{P}_{ij}(\vec{r}_{ij}) \vec{\theta}_{ij}, \quad (15)$$

where  $\zeta$  and  $\sigma$  are the friction constant and the noise strength, respectively. Here  $\overset{\leftrightarrow}{P}_{ij}(\vec{r}_{ij})$  is a projection operator

$$\overset{\leftrightarrow}{P} = \overset{\leftrightarrow}{P}^T = \overset{\leftrightarrow}{P}^2, \quad (16)$$

which is symmetric in the particle indices ( $\overset{\leftrightarrow}{P}_{ij} = \overset{\leftrightarrow}{P}_{ji}$ ).

The noise vector  $\vec{\theta}_{ij}$

$$\langle \vec{\theta}_{ij}(t) \otimes \vec{\theta}_{kl}(t') \rangle = 2 \overset{\leftrightarrow}{I} (\delta_{ik} \delta_{jl} - \delta_{il} \delta_{jk}) \delta(t - t') \quad (17)$$

is antisymmetric in the particle indices ( $\vec{\theta}_{ij} = -\vec{\theta}_{ji}$ ). The fluctuation-dissipation theorem is thus satisfied. If we choose the projector along the interatomic axis between particle  $i$  and  $j$   $\overset{\leftrightarrow}{P}_{ij}(\vec{r}_{ij}) = \hat{r}_{ij} \otimes \hat{r}_{ij}$ , we

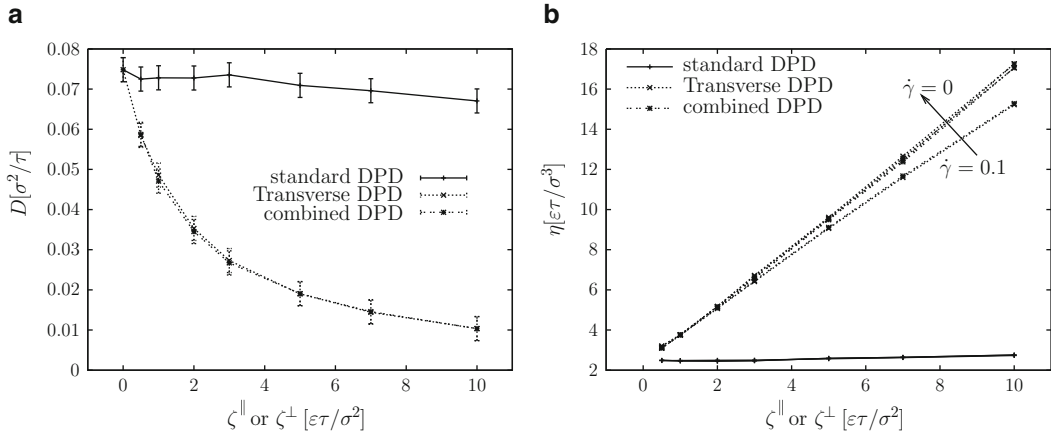


Fig. 8. Tuning the transport coefficients using transverse DPD thermostat. The figure is taken from (24). Reproduced by permission of The Royal Society of Chemistry. (a) Diffusion constant (b) Shear viscosity.

obtain the standard DPD thermostat, whereas  $\overleftrightarrow{P}_{ij}(\vec{r}_{ij}) = \overleftrightarrow{I} - \hat{r}_{ij} \otimes \hat{r}_{ij}$  yields the Transverse DPD thermostat.

As it turns out, the transport coefficient is rather insensitive to the value of the friction constant for damping the central relative velocities using the standard DPD thermostat. However, they are very sensitive to the value of the friction constant for damping the transverse relative velocities with the Transverse DPD thermostat as Fig. 8 shows (24).

### 3. AdResS: Technical Implementation

Very recently the AdResS scheme has been included into an open-source package ESPResSo for soft matter simulations (41, 42). This flexible implementation of AdResS will allow the simulation community to easily adapt the AdResS setup for their particular problems of interest. We hope and envisage that this will further boost the usage of AdResS.

### 4. Extension to Continuum Resolution

Recently, we have extended the AdResS scheme with the continuum description of a liquid modeled by the Navier-Stokes equation (10, 15). The triple-scale scheme was derived by combining two dual-scale schemes: AdResS, which couples the atomic and coarse-grained scales within a molecular dynamics (MD) simulation

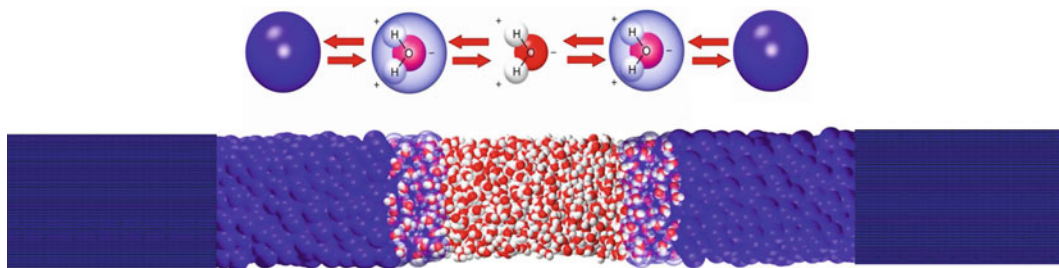


Fig. 9. The triple-scale model of liquid water (15).

framework, and a hybrid flux-exchange based continuum-MD scheme (HybridMD) developed by Delgado-Buscalioni et al. (43). The resulting triple-scale model consists of a particle-based micro-mesoscale MD region, which is divided into a central atomistic and a surrounding mesoscopic domain, and a macroscopic region modeled on the hydrodynamic continuum level as presented in Fig. 9 for liquid water. The central idea of the triple-scale method is to gradually increase the resolution as one approaches to the region of interest, that is, the atomistic region. The continuum and MD domains exchange information via mass and momentum fluxes. These fluxes are conserved across the interface between continuum and MD regions. The triple-scale approach is designed for molecular simulations of open domains with relatively large molecules, either in the grand canonical ensemble or under nonequilibrium conditions.

---

## 5. Extension to Quantum Level

A special treatment deserves the conceptual extension of AdResS to quantum problems. In general an adaptive approach that allows to pass from a quantum to a classical description and vice versa would require more than the mere change of number of DOFs. It requires the smooth passage from different kinds of physical principles. In fact while classical mechanics is governed by a deterministic evolution, quantum mechanics is characterized by the probabilistic character. For systems where electrons are explicitly treated, a classical-quantum adaptive scheme properly based on the Schrödinger equation would lead to the problem of variable number of particles, that is a varying particle normalization condition as the system evolves. So far schemes that treat electrons adaptively are based on practical solutions and not on a complete and consistent theoretical framework (6, 44). Instead if the quantum particles are the atoms (without considering explicitly the electrons), then the quantum problem, for some properties, can be mapped on an effective classical one. In this case, as a matter of fact, the adaptive coupling occurs between classical descriptions. The idea of

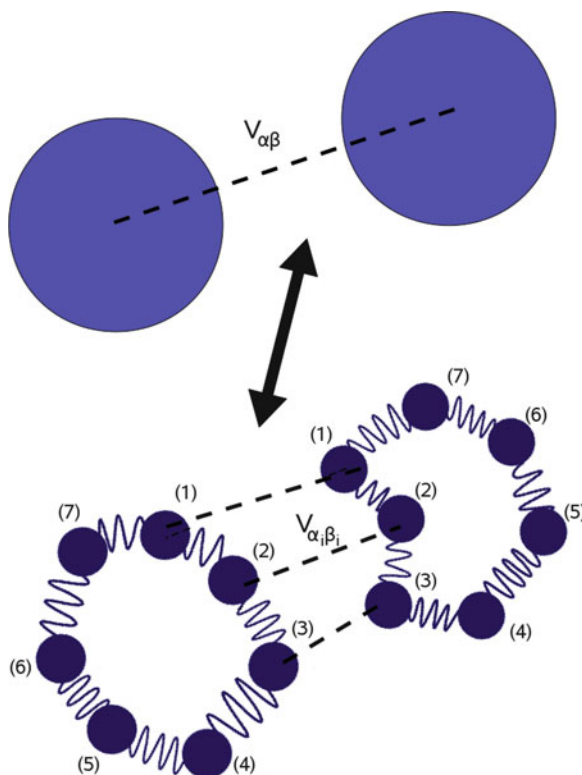


Fig. 10. Pictorial representation of the idea of path integral description of atoms. Two atoms,  $\alpha$  and  $\beta$  interacting in the classical approach as rigid spheres become two polymer rings whose interatomic classical interaction is distributed over pairs of beads  $\alpha_i\beta_i$ . The neighboring beads  $i, i + 1$  (and  $i, i - 1$ ) are kept together by an elastic potential whose constant depends on the temperature of the system. The delocalization of the atoms onto several beads characterizes its quantum nature.

quantum atoms is based on the path-integral description (45); this latter describes the quantum atoms as classical polymer rings; in this context, the beads of a polymer ring are fictitious classical particles, as presented in Fig. 10. The simulation can then be performed adaptively so that one can have an atomistic or coarse-grained resolution in one region and a path-integral resolution, where each atom is represented by a polymer ring, in another with free exchange between the two regions. In this situation, the principles of AdResS apply straightforwardly as to the case of two classical regions characterized by different numbers of DOFs. The application to study the equilibrium statistical properties of a liquid of tetrahedral molecules has shown that indeed this idea is rather robust both conceptually and numerically (8) (see “quantum to classical” part of Fig. 1).

---

## 6. Conclusions and Outlook

The development of AdResS is a subject of growing interest within the community of condensed matter, material science, and chemical physics. The interest in this kind of approach rises from the fact that, as discussed in this chapter, it may efficiently tackle the problem of interplay between different scales. This occurs by properly treating, simultaneously, all the relevant molecular DOF in each region of the simulation box and, because of the free diffusion of molecules from one region to another, properly accounting for density fluctuations. The practical consequences are an optimal employment of computational resources and an efficient analysis of the simulation data. In fact it allows for the reduction of computational costs by treating high-resolution models, which are computationally demanding, only in restricted regions and at the same time assures that details not relevant for the problem are not processed in regions where high resolution is not required. These last aspects allow in turn to derive a clear understanding of the basic physical features characterizing a given problem, avoiding that an excess of details overshadows the essential physics. In this sense, multiscale approaches as AdResS will allow not only to treat problem that before were prohibitive but also understand how the different scales, expressed by the molecular resolutions interfaced, are connected to each other. For example, in the solvation of a molecule, one may be interested to understand to which extent the local hydrogen bond network in the hydration shell is influenced by that of the bulk. To this aim one may employ AdResS as an analysis tool and perform simulations with varying sizes of the atomistic region interfaced with a coarse-grained region or even with the continuum where hydrogen bonds are not present. Depending on the minimum size of the atomistic region required to properly reproduce hydration properties, one can then comment on the extension of the influence of the hydrogen bond network on the hydration shell (46). In a similar spirit, one may think of the capture or release of a proton from a solvated molecule; in this case the quantum mechanical behavior of the proton passage would be described by, for example, the path-integral approach in a small region, while the large surrounding of bulk water can be represented with a coarser resolution. By further extending the AdResS methodology to continuum, one can go beyond equilibrium molecular dynamics simulations using periodic boundary conditions and study nonequilibrium processes, for example, fluid flows relevant for nanofluidics applications.

## Acknowledgements

Over the years we have collaborated with many colleagues and students on the topics described in this chapter. Out of them we would like to especially thank K. Kremer, R. Delgado-Buscalioni, C. Junghans, A. B. Poma, S. Poblete, C. Clementi, B. Lambeth, and S. Matysiak for fruitful collaboration and many discussions.

## References

- Rafii-Tabar H, Hua L, Cross M (1998) A multi-scale atomistic-continuum modelling of crack propagation in a two-dimensional macroscopic plate. *J Phys: Condens Matter* 10:2375–2387
- Broughton JQ, Abraham FF, Bernstein N, Kaxiras E (1999) Concurrent coupling of length scales: methodology and application. *Phys Rev B* 60:2391–2403
- Hadjiconstantinou NG (1999) Combining atomistic and continuum simulations of contact-line motion. *Phys Rev E* 59:2475–2478
- Smirnova JA, Zhigilei LV, Garrison BJ (1999) A combined molecular dynamics and finite element method technique applied to laser induced pressure wave propagation. *Comput Phys Commun* 118:11–16
- Rottler J, Barsky S, Robbins MO (2002) Cracks and crazes: on calculating the macroscopic fracture energy of glassy polymers from molecular simulations. *Phys Rev Lett* 89:148304
- Csanyi G, Albaret T, Payne MC, DeVita A (2004) 'Learn on the fly': a hybrid classical and quantum-mechanical molecular dynamics simulation. *Phys Rev Lett* 93:175503
- Heyden A, Lin H, Truhlar DG (2007) Adaptive partitioning in combined quantum mechanical and molecular mechanical calculations of potential energy functions for multiscale simulations. *J Phys Chem B* 111:2231–2241
- Poma AB, Delle Site L (2010) Classical to path-integral adaptive resolution in molecular simulation: towards a smooth quantum-classical coupling. *Phys Rev Lett* 104:250201
- Praprotnik M, Delle Site L, Kremer K (2005) Adaptive resolution molecular dynamics simulation: changing the degrees of freedom on the fly. *J Chem Phys* 123:224106
- Delgado-Buscalioni R, Kremer K, Praprotnik M (2008) Concurrent triple-scale simulation of molecular liquids. *J Chem Phys* 128:114110
- Praprotnik M, Delle Site L, Kremer K (2008) Multiscale simulation of soft matter: from scale bridging to adaptive resolution. *Annu Rev Phys Chem* 59:545–571
- Poblete S, Praprotnik M, Delle Site L, Kremer K (2010) Coupling different levels of resolution in molecular simulations. *J Chem Phys* 132:114101
- Praprotnik M, Delle Site L, Kremer K (2006) Adaptive resolution scheme (address) for efficient hybrid atomistic/mesoscale molecular dynamics simulations of dense liquids. *Phys Rev E* 73:066701
- Praprotnik M, Matysiak S, Delle Site L, Kremer K, Clementi C (2007) Adaptive resolution simulation of liquid water. *J Phys: Condens Matter* 19:292201
- Delgado-Buscalioni R, Kremer K, Praprotnik M (2009) Coupling atomistic and continuum hydrodynamics through a mesoscopic model: application to liquid water. *J Chem Phys* 131:244107
- Praprotnik M, Kremer K, Delle Site L (2007) Adaptive molecular resolution via a continuous change of the phase space dimensionality. *Phys Rev E* 75:017701
- Klapp SHL, Diestler DJ, Schoen M (2004) Why are effective potentials 'soft'? *J Phys: Condens Matter* 16:7331–7352
- Nonnenmacher TF (1990) Fractional integral and differential equations for a class of Levi-type probability densities. *J Phys A: Math Gen* 23:L697S–L700S
- Hilfer R (ed) (2000) Applications of fractional calculus in physics. World Scientific Publishing, Co. Pte. Ltd, Singapore
- Cottrill-Shepherd K, Naber M (2001) Fractional differential forms. *J Math Phys* 42:2203–2212
- Tarasov VE (2004) Fractional generalization of Liouville equations. *Chaos* 14:123–127
- Tarasov VE (2005) Fractional systems and fractional Bogoliubov hierarchy equations. *Phys Rev E* 71:011102
- Praprotnik M, Kremer K, Delle Site L (2007) Fractional dimensions of phase space variables:

- a tool for varying the degrees of freedom of a system in a multiscale treatment. *J Phys A: Math Theor* 40:F281–F288
24. Junghans C, Praprotnik M, Kremer K (2008) Transport properties controlled by a thermostat: an extended dissipative particle dynamics thermostat. *Soft Matter* 4:156–161
  25. Delle Site L (2007) Some fundamental problems for an energy-conserving adaptive-resolution molecular dynamics scheme. *Phys Rev E* 76:047701
  26. Janežič D, Praprotnik M, Merzel F (2005) Molecular dynamics integration and molecular vibrational theory: I. New symplectic integrators. *J Chem Phys* 122:174101
  27. Soddemann T, Dünweg B, Kremer K (2003) Dissipative particle dynamics: a useful thermostat for equilibrium and nonequilibrium molecular dynamics simulations. *Phys Rev E* 68:046702
  28. Praprotnik M, Delle Site L, Kremer K (2007) A macromolecule in a solvent: adaptive resolution molecular dynamics simulation. *J Chem Phys* 126:134902
  29. Matysiak S, Clementi C, Praprotnik M, Kremer K, Delle Site L (2008) Modeling diffusive dynamics in adaptive resolution simulation of liquid water. *J Chem Phys* 128:024503
  30. Henderson RL (1974) A uniqueness theorem for fluid pair correlation functions. *Phys Lett* 49A:197–198
  31. Soper AK (1996) Empirical monte carlo simulation of fluid structure. *Chem Phys* 202:295–306
  32. Tschöp W, Kremer K, Hahn O, Batoulis J, Bürger T (1998) Simulation of polymer melts. II. From coarse-grained models back to atomistic description. *Acta Polym* 49:75–79
  33. Reith D, Pütz M, Müller-Plathe F (2003) Deriving effective mesoscale potentials from atomistic simulations. *J Comput Chem* 24:1624–1636
  34. Lyubartsev AP, Laaksonen A (1995) Calculation of effective interaction potentials from radial distribution functions: a reverse monte carlo approach. *Phys Rev E* 52:3730–3737
  35. Izvekov S, Parrinello M, Burnham CB, Voth GA (2004) Effective force fields for condensed phase systems from ab initio molecular dynamics simulation: a new method for force-matching. *J Chem Phys* 120:10896–10913
  36. Izvekov S, Voth GA (2005) Multiscale coarse graining of liquid-state systems. *J Chem Phys* 123:134105
  37. Mullinax JW, Noid WG (2009) Generalized yvon-born-green theory for molecular systems. *Phys Rev Lett* 103:198104
  38. Mullinax JW, Noid WG (2009) Extended ensemble approach for deriving transferable coarse-grained potentials. *J Chem Phys* 131:104110
  39. Wang H, Junghans C, Kremer K (2009) Comparative atomistic and coarse-grained study of water: what do we lose by coarse-graining? *Eur Phys J E* 28:221
  40. Español P, Warren P (1995) Statistical mechanics of dissipative particle dynamics. *Europhys Lett* 30:191–196
  41. Limbach HJ, Arnold A, Mann BA, Holm C (2006) Espresso—an extensible simulation package for research on soft matter systems. *Comput Phys Comm* 174:704–727 <http://www.espresso.mpg.de>
  42. Junghans C, Pobleto S (2010) A reference implementation of the adaptive resolution scheme in espresso. *Comput Phys Comm* 181:1449
  43. Fabritiis GD, Delgado-Buscalioni R, Coveney PV (2006) Multiscale modeling of liquids with molecular specificity. *Phys Rev Lett* 97:134501
  44. Bulo R, Ensing B, Vischer L (2009) Toward a practical method for adaptive qm/mm simulations. *J Chem Theor Comp* 5:2212
  45. Tuckermann M (2002) Path integration via molecular dynamics. Quantum simulations of complex many-body systems: from theory to algorithms, NIC Series, John von Neumann Institute for Computing, pp 269–298
  46. Bradley P, Lambeth, Christoph Junghans, Kurt Kremer, Cecilia Clementi, and Luigi Delle Site (2010): On the Locality of Hydrogen Bond Networks at Hydrophobic Interfaces *J Chem Phys* 133:221101